ADAPTIVE POLISHED ROD VELOCITY PROFILE SELECTION AND PUMP CARD EVALUATION

Kalpesh Singal, Abhijit Khare, Justin E. Barton, Omar Al Assad and Shyam Sivaramakrishnan
GE Global Research Center

David W. Doyle, Qing Wu, Michael Honey, Darrell Stubblefield, Terry Stephenson
GE Lufkin Rod Lift Systems

ABSTRACT

While controllers for VSD-driven pumping units have the capability today to make manually programmed intra-stroke speed changes, they do not autonomously make these decisions. This work will describe a new control algorithm that autonomously chooses polished rod velocity profiles to maximize efficiency and production while protecting pumping units and rods from overloads. The algorithm uses surface and downhole cards from the earlier stroke, generating a new polished rod velocity profile for the following stroke. In particular, the algorithm modulates ramp rates and peak velocities of a smooth 'trapezoidal' velocity profile. Simulations of this algorithm suggest that load violations can be corrected, while optimizing production and efficiency. In order to diagnose changes to pump cards in real-time, two approaches will be compared, namely the analytical Fourier Series method and the numerical finite difference method. It will be shown that the real-time performance of both approaches is largely identical.

Keywords: Adaptive control, intra stroke, optimization, Fourier Series, finite difference

INTRODUCTION

Automated operation of rod pumps is now several decades old with a typical goal being increasing longevity of pump and downhole equipment like sucker rods and tubing. Rod pump controllers normally monitor pump fillage i.e. percentage of liquid in total volume of pump and maintain stroking speed to ensure fillage never decreases below a set point. In contrast, when fillage is found to be high, controllers speed up stroking to increase production, until a certain maximum strokes per minute (SPM) limit is reached. In this process, the 'shape' of a rod pump's velocity profile never changes; however, the velocity profile may shrink and expand depending on the number of pumping strokes per minute.

Such an automation strategy effectively maintains life of pumping unit and downhole equipment by preventing fluid pound events and shock loads. However, such a strategy does not enhance production efficiency and capacity of installed pumping units. In this paper, an enhanced automation strategy will be described, that alters the polished rod velocity profile within a stroke (intra-stroke). It will be shown with simulation examples that such an automation strategy can reduce operating costs and increase operating margins by increasing production efficiency and capacity. Indeed, any control of pumping unit velocity profiles would require a variable speed drive (VSD) to control the pumping unit's motor. Hence, the proposed approach is only relevant for VSD-driven pumping units.

EFFECT OF POLISHED ROD VELOCITY PROFILES

Polished rod velocity profiles affect production, efficiency and peak loads of a rod pumping system as described below. Using this understanding, it is possible to develop an automated control strategy that simultaneously optimizes production, efficiency and peak loads.

PRODUCTION

Polished rod velocity profiles control effective downhole stroke of a rod pumping system at any given surface stroke length, which in turn controls production rate. To understand the effect of polished rod velocity profile on downhole stroke, a frequency response plot is useful. Figure 1 shows a typical frequency response plot with y-axis being ratio of downhole stroke to surface stroke and x-axis being ratio of operating strokes per minute to natural frequency of sucker rod assembly. Figure 1 shows that a peak may be seen close to the natural frequency of the system, which normally varies between 20 to 100 SPM depending on depth of well. Noting that most beam pumps operate at speeds less than 13 SPM, the section of curve to the left of resonance point is of interest.

Any polished rod velocity profile comprises of a sum of low frequency and high frequency components. The dominant frequency component would have a frequency equal to the operating SPM while smaller amplitude components will be composed of higher frequencies. Figure 1 shows that higher frequency components will be amplified downhole. Thus, one approach to increase downhole stretch is to increase the magnitude of high frequency components. This in turn can be achieved by ramping up/down velocities quickly. It must be noted that effective downhole stretch is also dependent on phase of all frequency components. However, it is a good rule of thumb that increasing amplitude of higher frequency content increases downhole stretch.

Taking this analysis to velocity profiles of beam pumps, it is possible to see how velocity profiles of beam pumps leave room for improvement. It is well-known that beam pumps create approximately sinusoidal polished rod velocity profiles. Such velocity profiles largely consist of a single dominant frequency equal to the operating strokes per minute with little high frequency components. Figure 2 shows results from simulations of a beam pump operating at 7.7 SPM using a purely sinusoidal velocity profile and its effect on the surface and downhole cards. It can be seen from the downhole card shown at bottom of plot that:

a) the downhole plunger displacement is approximately 85 inches and
b) the surface card shown at top of plot touches the permissible load envelope shown as dashed lines.
c) Net production was computed to be 120 barrles per day (BPD).

In contrast, when the same system operates with a velocity profile resembling a smooth trapezoid at 7.7 SPM,

a) higher downhole plunger displacement of approximately 92 inches is possible as shown in Figure 3. This higher downhole displacement increases net production by ~10%, thereby increasing production capacity of the installed rod pump system. It must be noted here that additional power will be required at the surface to produce this extra amount.
b) Further, the surface card no longer touches the permissible load envelope and allows stroking rate to be increased to a maximum value of 10.8 SPM as shown in Figure 3, effectively increasing production by ~50% or 188 BPD.

Thus, a goal of velocity profile adaptation needs to be increasing amplitude of higher frequency content or increasing acceleration/deceleration in velocity profiles, which in turn leads to increased production.

EFFICIENCY

The overall efficiency of rod pumping is controlled by losses occurring throughout the tubing section which include viscous drag losses of fluid relative to tubing walls as well as sucker rods moving through fluid. Both these losses are dependent on velocities achieved by fluids and rods during operation. Indeed, such losses are typically proportional to approximately second to third power of polished rod velocity; implying that higher peak velocities in a velocity profile cause much steeper losses. In order to reduce such losses, it is required to maintain as low a velocity for as long as possible through the velocity profile. This in turn can be achieved by using a trapezoidal velocity profile with a flat velocity section and fast acceleration. Hence, the method for increasing system efficiency matches the method for increasing production.

LOADS AND TORQUES

Along with impact on production and efficiency, velocity profiles have a large impact on structural loads and gearbox torques handled by pumping units. Loads and torques are affected as follows by velocity profiles:

a) Velocity profiles with faster ramp rates create larger surface loads (and hence large gearbox torques) during accelerations and decelerations. This is a direct result of needing to move inertias faster.
b) In general, velocity profiles with faster ramp rates also cause larger stress waves through the rod string, thereby increasing peak loads on pumping unit. However, a velocity profile at the same SPM with a faster ramp rate would also typically have a smaller peak velocity, which would bring down the peak acceleration needed.

Thus, loads and torques can typically be reduced by reducing accelerations and decelerations in velocity profiles. Indeed, this is in contrast to the need for accelerating and decelerating faster for increasing production and efficiency. Thus, to optimize production, efficiency and pump loads, accelerations and decelerations need to be increased as much as allowed by load limits and stopped when load limits are approached.

Finally, a velocity profile need not look symmetric as shown above and may be adjusted to reduce load spikes in specific regions of the surface card to reduce loading on gear reducer, structure and rods.

ADAPTIVE VELOCITY PROFILE CONTROL ALGORITHM

Based on above insights, it is possible to develop algorithms that automatically adjust ramp rates of trapezoidal velocity profiles to maximize production, efficiency and equipment life. A possible algorithm would be one similar to current pump-off control algorithms which reduce SPM when downhole pump is partially full. However, once the downhole pump is fully filled with liquid, such an algorithm would seek to increase SPM until a load constraint is reached. Once a load constraint is reached, the algorithm would not immediately reduce SPM. Rather, it would adjust relevant ramp rate in a trapezoidal velocity profile to reduce loads. It would continue to adjust ramp rates until load constraints are not reached or a limit on number of strokes is met. If it encounters a limit on number of strokes, it would reduce SPM and repeat the process. Repeating this process continuously would lead to a velocity profile customized for any given well condition and pumping unit.

Figure 4 shows an algorithm that accomplishes the above. Such an algorithm was tested using simulations of varying well conditions as well as on a pumping unit under loads upto 30,000 lbf and found to be able to optimize production, efficiency and loads as expected.

IMPACT OF VARYING OPERATING CONDITIONS ON DETERMINATION OF PUMP CARD VIA DIAGNOSTIC ALGORITHMS

In order to be able to incorporate the concepts previously described to modify the polished rod velocity profile to improve pumping efficiency, production, and availability into a rod pump control algorithm as described in earlier sections, diagnostic algorithms need to be used to infer the current operating state of the pumping system from available measurements. In response to dynamically varying pump operating conditions, for example a decrease in pump fillage, the rod pump controller would alter the polished rod velocity profile to improve system performance. Therefore, a necessary requirement of the diagnostic algorithms is that they need to be able to accurately describe the state of the pumping system during dynamic variations in operating conditions, such as dynamic changes in the polished rod motion profile. The determination of the downhole pump card based on measured surface conditions is one of the most critical diagnostic algorithms for optimized rod pump operation.

In rod pump applications, the elastic behavior of the rod string is described by the well-known damped wave equation, which is derived from Newtonian mechanics and Hooke's law of elasticity. The wave equation is expressed as

$$a^2 \frac{\partial^2 u}{\partial x^2} = \frac{\partial^2 u}{\partial t^2} + c \frac{\partial u}{\partial t}$$

where u is the displacement of the rod, x is the spatial coordinate vertically along the rod, t is time, c is the viscous damping coefficient, and a is the acoustic velocity in the sucker rod medium. The diagnostic problem consists of calculating the downhole pump load and position based on the measured polished rod load and position. There are two main mathematical approaches currently used in the industry to solve this diagnostic problem, the analytical Fourier Series method [1] and the numerical finite difference method [2]. The Fourier Series approach is predicated on the analytical solution of the wave equation by using a mathematical technique referred to as separation of variables to solve the partial differential equation. This analytical solution takes the form of an infinite Fourier Series, and in order to obtain it, the simplifying assumption of steady-state pump operating conditions is applied. For practical computational implementation, only a finite number of terms are retained in the solution, and the coefficients in the truncated Fourier Series are calculated so that the solution satisfies the measured surface load and position boundary conditions. This analytical solution can then be used to obtain the load and displacement at any depth along the rod string. The finite difference approach is based on a numerical method to integrate the wave equation to obtain an approximate solution of the partial differential equation which relaxes the assumption of steady-state pump operating conditions that is needed to obtain the Fourier Series solution. To facilitate this numerical solution, the rod string is spatially discretized into smaller elements whose interfaces are referred to as nodes. The dynamic behavior of the rod string is then approximated by replacing the partial derivatives in the wave equation with their finite difference analogs to obtain an algebraic equation for the nodal displacements. The load and displacement along the rod string is then obtained by recursively solving this algebraic equation for successive nodal displacements, where the measured surface load and position are used as inputs.

In order to discern the ability of these two diagnostic approaches to accurately compute the pump card under dynamic variations in pump operating conditions, three simulation scenarios are studied:

1.) Constant surface motion profile shape and stroke speed with changing downhole conditions on consecutive strokes
2.) Constant downhole conditions and surface motion profile shape with changing stroke speed on consecutive strokes
3.) Constant downhole conditions and stroke speed with changing surface motion profile shape on consecutive strokes.

The simulations are generated as follows. A predictive simulation model is used to calculate surface load, pump position, and pump load from known surface position. The predictive model is comprised of a model of the rod dynamics that is coupled with a model of the downhole pump. The model of the downhole pump predicts pump load based on a feedback signal of the pump position that is calculated by the model of the rod dynamics. The predicted surface card is then used as an input to both the Fourier Series and finite difference algorithms to calculate the diagnostic pump cards. Finally, the pump cards computed with the diagnostic algorithms are compared to the pump card generated by the predictive simulation. The testing conditions are for a 2 in. pump with a four taper rod string with the following characteristics:

1.) Polished rod: 1.5 in. diameter, 26 ft. length
2.) D-grade sucker rod: 1 in. diameter, 1500 ft. length
3.) D-grade sucker rod: 0.875 in. diameter, 1500 ft. length
4.) D-grade sucker rod: 0.75 in. diameter, 1175 ft. length
5.) D-grade sucker rod: 1.625 in. diameter, 200 ft. length.

The diagnostic solver configurations are:

1.) Fourier Series: 14 load Fourier coefficients, 6 position Fourier coefficients, sampling rate of 200 surface load and position pairs per stroke.
2.) Finite difference: Element size of approximately 30 ft., sampling time of 5 ms.

The results of the three simulation studies are shown in Figures 5-7. In the first simulation case, the pump fillage is changed from approximately 100% to 70% between stroke 1 and stroke 2, as shown in Figure 5. In the second simulation case, the stroke speed is changed from 3 strokes per minute to 5 strokes per minute between stroke 1 and stroke 2, as shown in Figure 6. In the third simulation case, the shape of the polished rod velocity profile is changed between stroke 1 and stroke 2, as shown in Figure 7. By comparison of the black line (finite difference) and circles (Fourier Series) with the light gray line (predicted) in Figure 5(middle and right), Figure 6(middle and right), and Figure 7(middle and right), it is observed that both diagnostic solutions demonstrate a high degree of accuracy in the computation of the pump card in the presence of dynamic variations in the operating conditions of the pumping system. Additionally, despite their fundamental mathematical differences, both the Fourier Series and finite difference computational approaches produce nearly identical diagnostic solutions of the wave equation to obtain the pump card. As a result, in practice either method could be used in a rod pump controller to provide diagnostic information to an adaptive polished rod velocity profile shaping control algorithm.

CONCLUSION

Overall, it was found that polished rod velocity profiles could be manipulated to optimize production capacity, efficiency and loads on pumping units. The developed algorithm for automating this process applies to any rod pumping unit using a VSD. Further, to aid the algorithm in assessing downhole pump behavior while velocity profiles were being changed, pump card calculation methods were evaluated for real-time response. It was found that both the Fourier Series and finite difference approaches were equally effective in monitoring the downhole pump card as velocity profile was varied.

REFERENCES

[1] Gibbs, S.G. and Neely, A.B.: “Computer Diagnosis of Down-Hole Conditions in Sucker Rod Pumping Wells,” JPT (Jan. 1666) 91-98: Trans., AIME, 237.

[2] Knapp, R.M.: “A Dynamic Investigation of Sucker-Rod Pumping,” MS Thesis, U. of Kansas, Topeka (Jan. 1969).

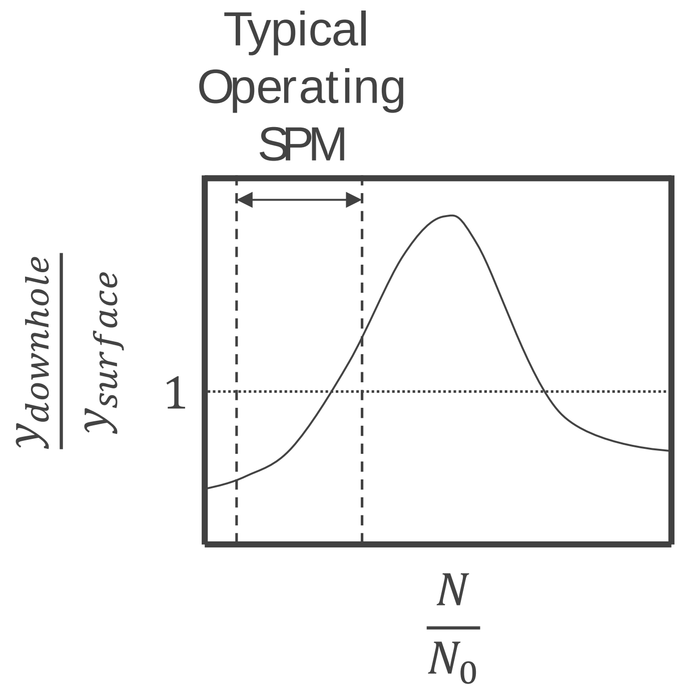

Figure 1 - Frequency response plot of downhole to surface stroke ratio as a function of specific speed

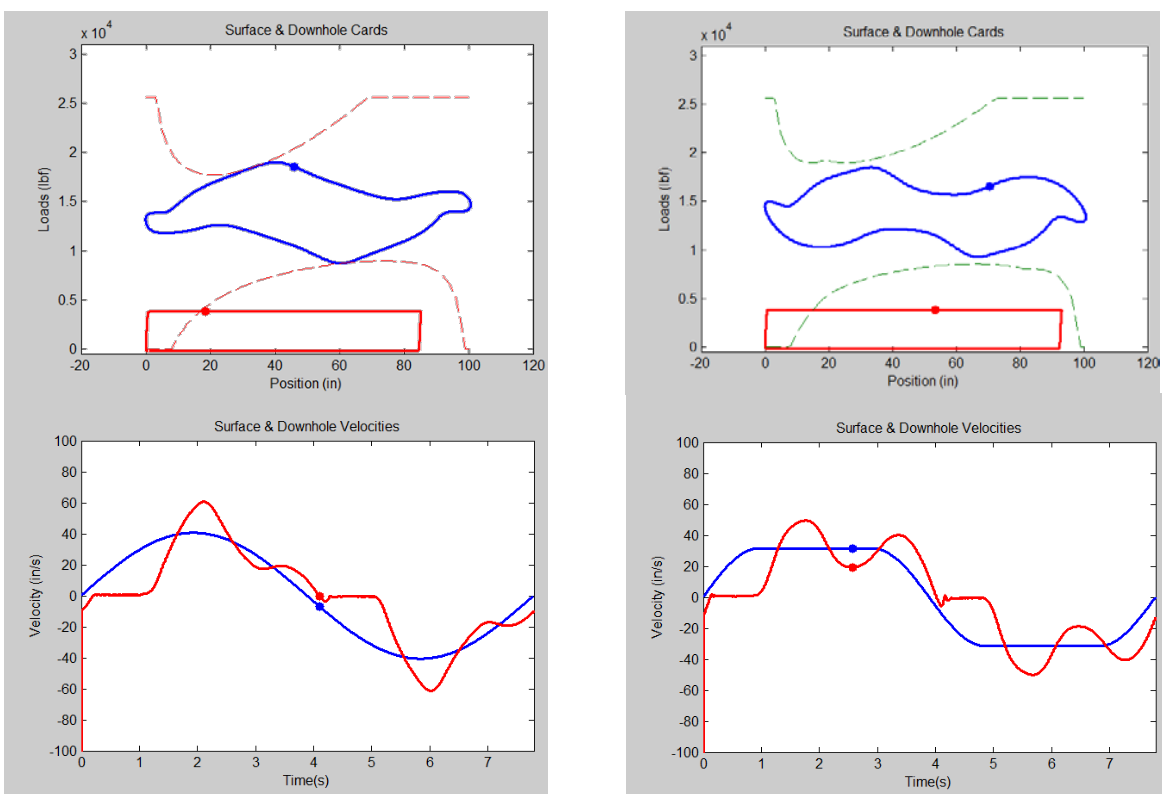

Figure 2 - Effect of sinusoidal (left) and trapezoidal (right) velocity profiles on surface cards and downhole stroke.

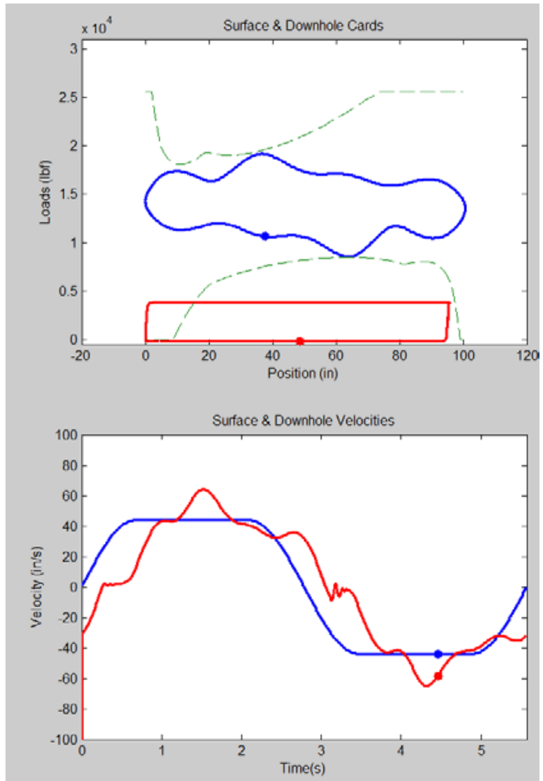

Figure 3 - System working at 10.8SPM before surface card touched permissible load envelope. Note that permissible load diagram was adjusted to account for inertial and speed variations.

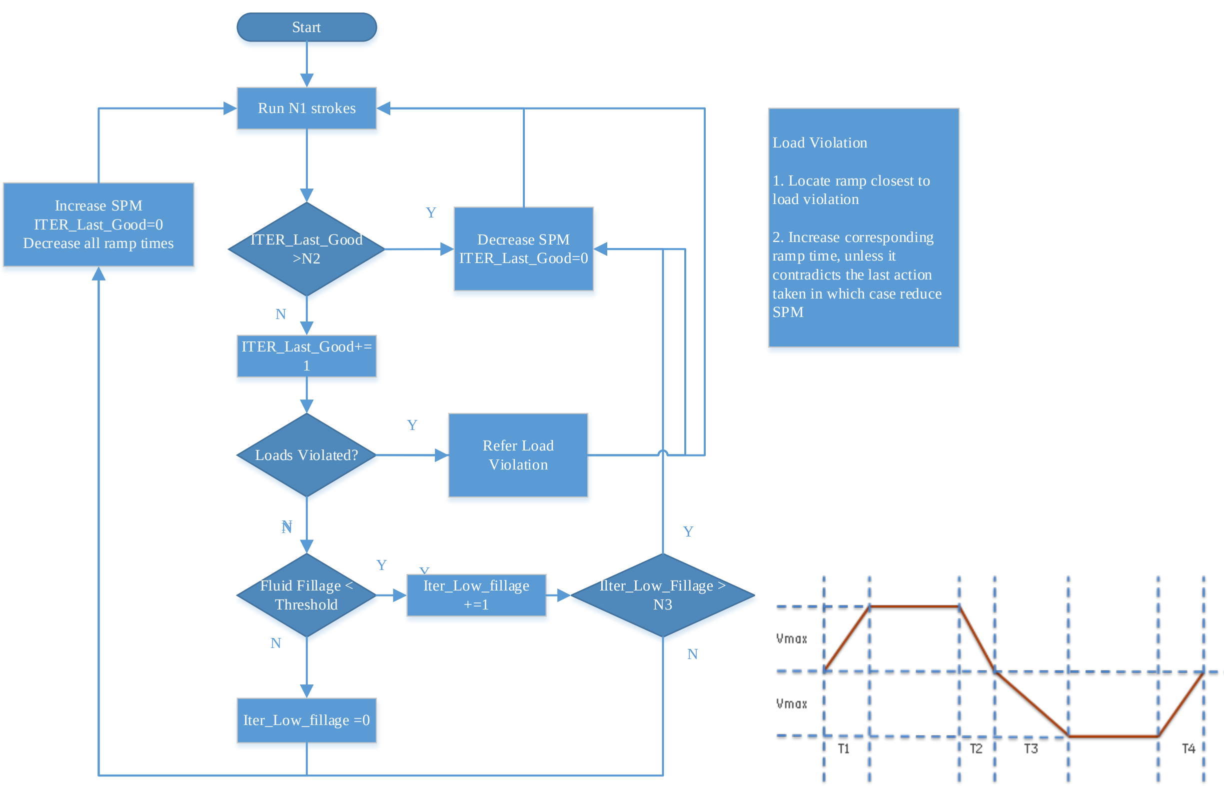

Figure 4 - Algorithm for automating velocity profile and SPM change in response to well conditions

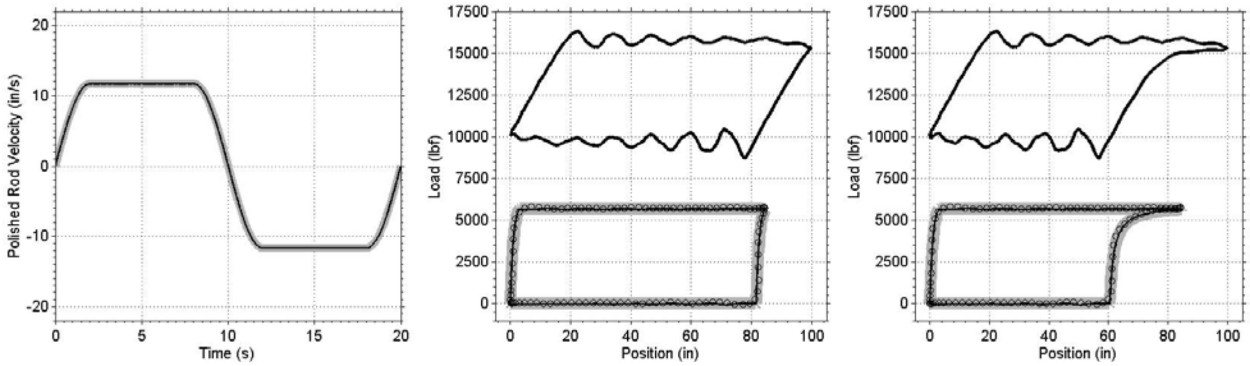

Figure 5 - Comparison of diagnostic pump card calculation methods for the first simulation scenario (changing pump fillage on consecutive strokes). The left figure shows the polished rod velocity profiles applied on consecutive strokes (light gray – stroke 1, black – stroke 2). The middle figure shows the surface and pump cards computed for stroke 1, and the right figure shows the surface and pump cards computed for stroke 2 (for pump cards: light gray – predicted, black – finite difference, circle – Fourier Series).

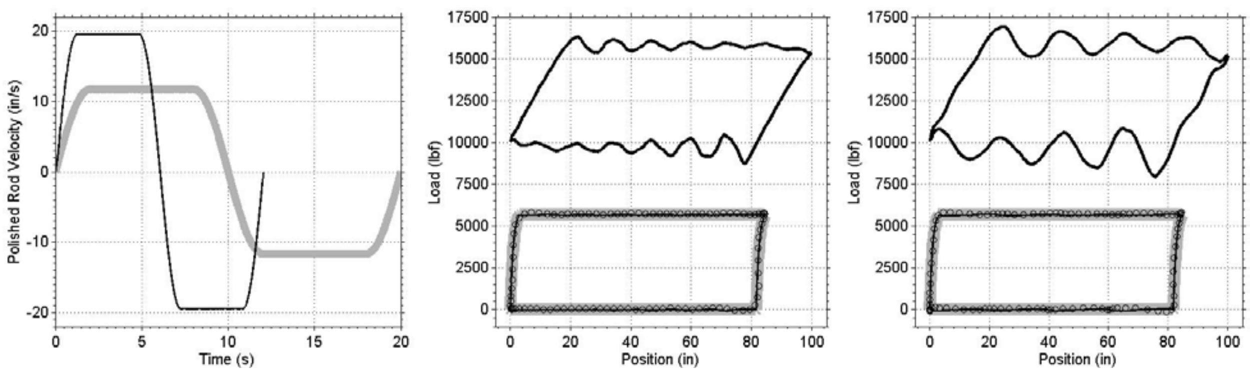

Figure 6 - Comparison of diagnostic pump card calculation methods for the second simulation scenario (changing stroke speed on consecutive strokes). The left figure shows the polished rod velocity profiles applied on consecutive strokes (light gray – stroke 1, black – stroke 2). The middle figure shows the surface and pump cards computed for stroke 1, and the right figure shows the surface and pump cards computed for stroke 2 (for pump cards: light gray – predicted, black – finite difference, circle – Fourier Series).

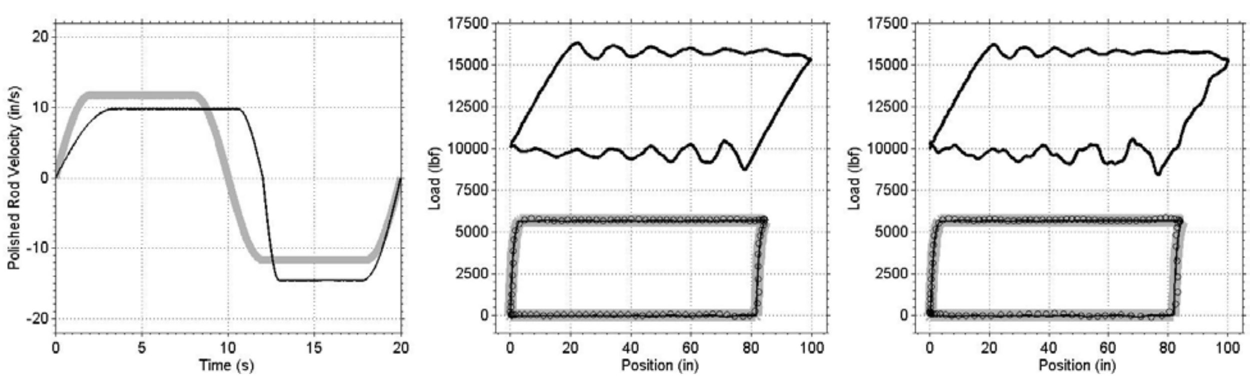

Figure 7: Comparison of diagnostic pump card calculation methods for the third simulation scenario (changing polished rod velocity profile on consecutive strokes). The left figure shows the polished rod velocity profiles applied on consecutive strokes (light gray – stroke 1, black – stroke 2). The middle figure shows the surface and pump cards computed for stroke 1, and the right figure shows the surface and pump cards computed for stroke 2 (for pump cards: light gray – predicted, black – finite difference, circle – Fourier Series).